1-1-2012

Preliminary Analysis of the Effects of Different Machining Techniques on Carbon Fibre Epoxy Materials

Diana Mollicone
Ryerson University

PRELIMINARY ANALYSIS OF THE EFFECTS OF DIFFERENT MACHINING TECHNIQUES ON CARBON FIBRE EPOXY MATERIALS

by

Diana Mollicone
B.A.Sc. - Materials Engineering
University of Toronto 2010

A project

presented to Ryerson University

in partial fulfillment of the

requirements for the degree of

Master of Engineering

in the Program of

Mechanical Engineering

Toronto, Ontario, Canada, 2012

Author’s Declaration

I Diana Mollicone, hereby declare that I am the sole author of this thesis. This is a true copy of the thesis, including any required final revisions, as accepted by my examiners.

I authorize Ryerson University to lend this thesis to other institutions or individuals for the purpose of scholarly research.

I further authorize Ryerson University to reproduce this thesis by photocopying or by other means, in total or in part, at the request of other institutions or individuals for the purpose of scholarly research.

I understand that my thesis may be made electronically available to the public.

Abstract

Preliminary Analysis of the Effects of Different Machining Techniques on Carbon Fibre Epoxy Materials

Master of Engineering 2012

Diana Mollicone

Mechanical Engineering

Ryerson University

Composite materials present a potential alternative to traditional metallic alloys in aerospace structural components such that they have desirable mechanical properties while possessing low densities. These components are traditionally joined together through bolts, which require the materials to have machined holes. This inquiry compared the effects of different types of machining on carbon epoxy plates: drilling with a coated bit and waterjet machining, and how they impact the material's behavior during load-bearing operations. Three forms of material testing were used: tensile testing, strain gauge, and infrared thermography analysis during cyclic loading. The results obtained do not demonstrate consistent patterns that would suggest that one machining method is beneficial over the other.

Acknowledgements

I would like to express my greatest gratitude towards Professor Habiba Bougherara for her thorough guidance throughout this project. It was with her patience and understanding nature that had me grasp the main objectives of this research topic. I'd like to thank her for allowing me to work independently so that I would not conflict with my full-time work schedule.

Members of the Bougherara group are extraordinary people. I'd like to give special thanks to two of her group members: Giovanni Montesano and Suraj Shah. Giovanni (John) was the main support behind all the experiments requiring thermographic strain gauge analysis and I'd like to thank him for stretching his schedule to guide me through the necessary experiments. Suraj guided me through the strain gauge testing, helped me to better understand the analysis procedure, and acted as the main liaison between the necessary laboratories and myself. Further, I'd like to thank another member of the Bougherara group, Muhammad Saleem Khan, whom is working on a similar project and freely shared his resources.

Furthermore, I'd like to thank my family and friends who are lucky to see my face for a full hour before I'm out the door again. Your moral support has been a tremendous help and knowing my parents are going to brag endlessly about my master's degree to extended family members gave me that extra incentive to do a great job.

Lastly, thank-you to Dr. Siyuan He and Dr. Ahmad Ghasempoor of Ryerson University's Department of Mechanical and Industrial Engineering for agreeing to attend my presentation. Thank you everyone.

THIS PAGE WAS LEFT INTENTIONALLY BLANK

Table of Contents

List of Figures

List of Units

°C	Degree centigrade
mm	Millimetre
MPa	Mega Pascal
N	Newtons
Hz	Hertz
s	Seconds
t	Time in seconds
m	Metre

List of Abbreviations

IRT	Infrared thermography
N	Number of cycles
N_f	Number of cycles until failure
D	Level of damage
D'	Cumulative Damage
E	Stiffness
E_0	Initial stiffness
E_f	Stiffness prior until failure
T	Temperature in degree centigrade
WC	Tungsten Carbide
TiN	Titanium Nitride

Nomenclature

L	Length of the plate
W	Width of the plate
T	Thickness of the plate
Δ	Change in property (usually temperature)
ε	Strain (mm/mm)
σ	Stress (MPa)

Chapter 1: Introduction and Scope

Composite materials possess several desirable properties when compared to conventional metals including higher specific strength, higher modulus, and better fatigue strength; all while maintaining a low density [1-3]. As a result, the use of composite materials has grown drastically, particularly in the fields of aerospace and aircraft for structural load-bearing applications [4]. Components comprised from composite materials are usually moulded to near-net shape, and machining is necessary for the final part assembly as aerospace components are joined through bolts and fasteners [5-6].

Conventional machining techniques such as drilling are used with composite materials because of the availability of equipment and knowledge of said methods [6-8]. However, when drilling composites, the main issue is the damage caused to the workpiece; the principal damage of concern is delamination and matrix cracking [7]. The focus of this paper is concerned with different forms of machining: drilling with a coated bit, and waterjet machining and how they behave in continuous load-bearing applications. Apparent advantages of waterjet machining include that it does not produce dust particles that are harmful when inhaled, it does not require finish sanding, and automation processes are easy to install [8-9].

The performance of the different machining methods have been evaluated through tensile testing, strain gauge testing, and infrared thermography. Tension tests were performed to gather basic mechanical properties of the materials as well as visual inspect the failure mechanism. Infrared thermography tests were used to gather a visual examination of the stress accumulation around the hole. Strain gauge tests were done to validate the numerical results obtained through infrared thermography.

Chapter 2: Literature Review

Experiments leading up to this inquiry include: the effects of stress concentrators in composite materials (including machined holes), the effects of drill bit coatings on machining, the advantages of non-traditional machining methods, the use of infrared thermography in composites analysis and the effects of ply stack-up in composite materials.

2.1 Stress Concentration in Composite Materials

Work done by S. D. Pandita et al. [10] investigated the tensile strain field of woven fabric composites in the presence of stress concentrations caused by geometrical defects, particularly circular and elliptical holes. Experiments were performed by placing plain woven composite plates in a tensile machine equipped with a strain mapping device and the plates were strained until failure. The experiments revealed that the strain concentrations are influenced by the tensile loading direction and the hole dimensions, which are defined as a height over width ratio or *b/a* [10].

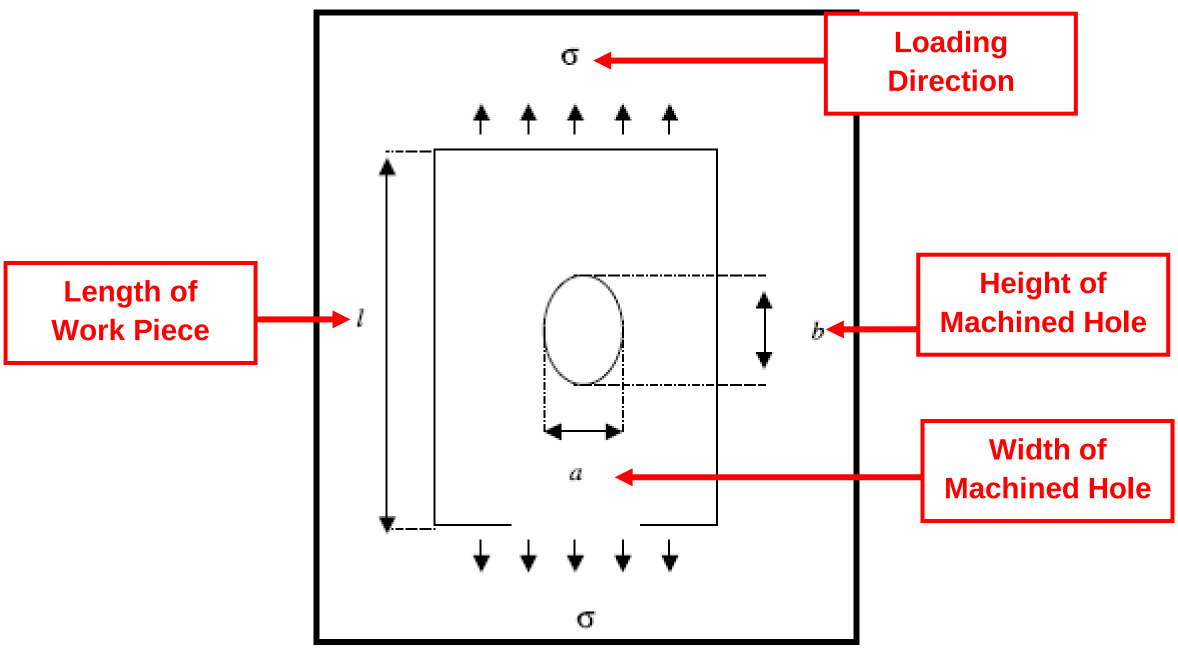

Figure 1: Labeled schematic of Pandita's workpiece [10]

Pandita's experiments [10] demonstrated that at lower shape parameters, the strain concentration is located at the tip of the elliptical holes. Increasing the shape parameter causes the stress concentration to become smaller because of the large perimeter for the stress to accumulate - allowing for higher stress value prior to fracture, as seen in Figure 2. When comparing failure modes though, it's apparent that lower (b/a) values fractured at mid-plane of the hole because the concentration is very sharp. Higher (b/a) values caused failures at other locations around the hole, Figure 3 illustrates the final failures of the work pieces. Larger (b/a) values increased the net strength slightly but the failure became less predictable.

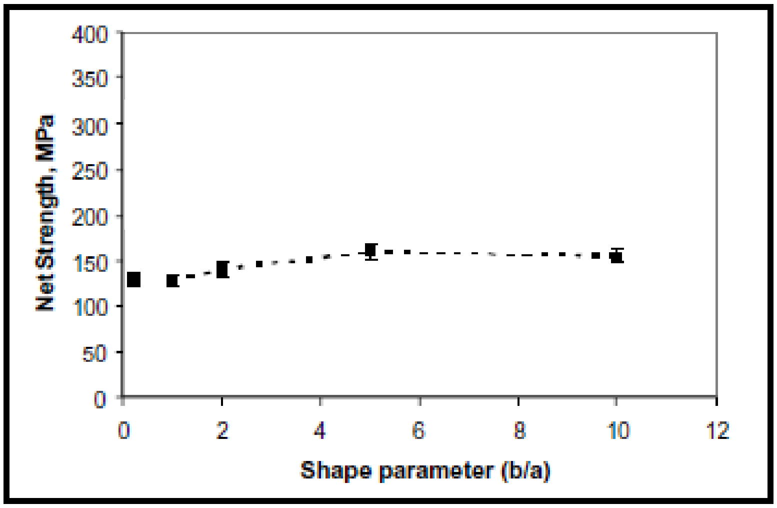

Figure 2: Residual Strength of Pandita's work pieces against the shape parameters [10]

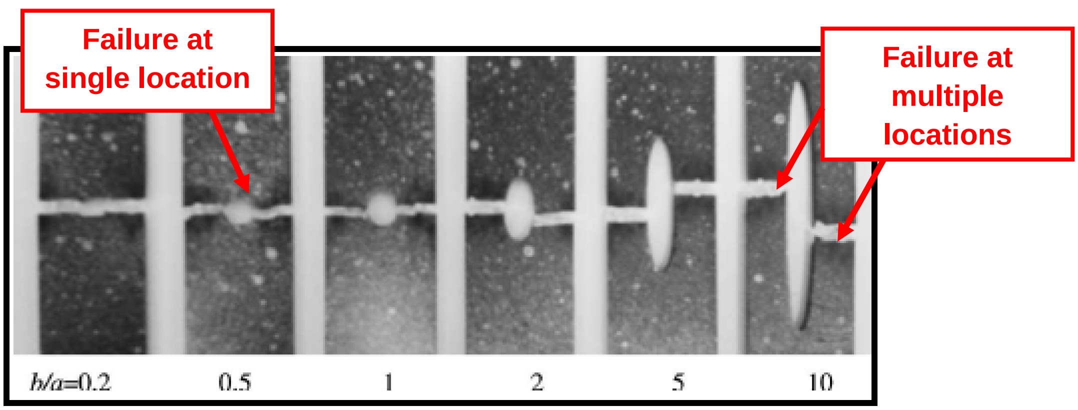

Figure 3: Final failure of elliptical holed specimens with different shape parameters after being subjected to uniaxial tension testing [10]

2.2 The Effects of Drill Bit Coatings

Experiments done by C. Murphy et al. [11] were concerned with the effect of coatings on the performance of traditional tungsten carbide (WC) drill bits used to drill carbon fibre-reinforced epoxy plates. The experiments made use of three different types of WC bits: uncoated, titanium nitride coated (TiN), and diamond-like carbon coating (DLC). The performance of the coatings has been analyzed in terms of damage to the composite and the thrust force.

Charles' experiments concluded that the use of coatings in the drill bits were found to be of no benefit when machining carbon-epoxy composites [11]. The damage done to composite materials during machining with drilling procedures is induced through delamination as the bit protrudes the last ply [11]. The coating serves to prolong the life of the bit itself [12-13].

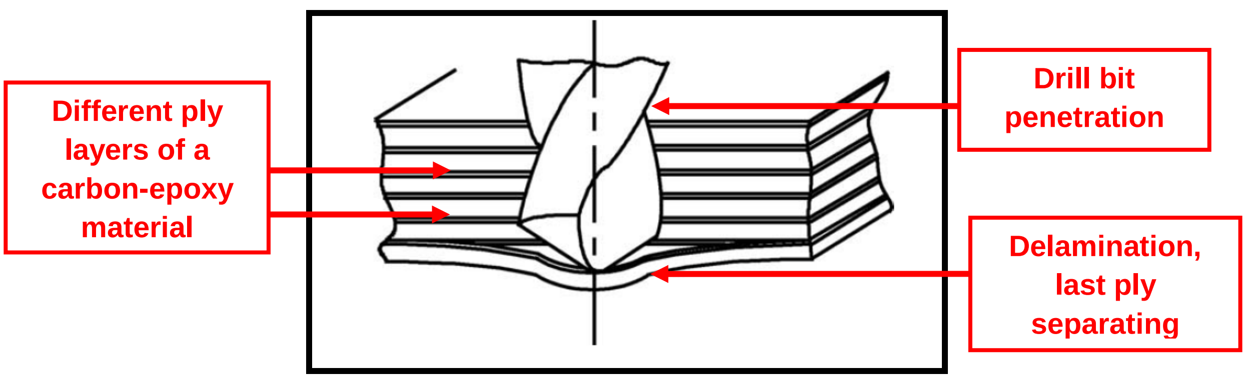

Figure 4: Schematic of delamination as the drill bit penetrates the last ply of a composite material [11]

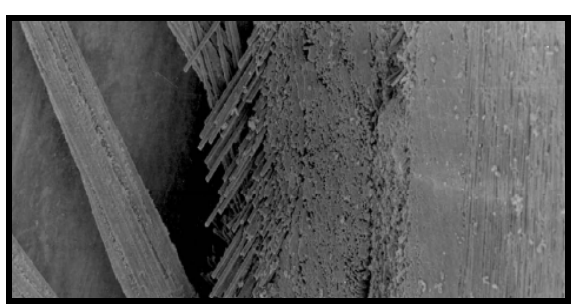

Figure 5: SEM image of delamination of the last ply caused by drilling [11]

2.3 Non-Traditional Drilling

Using C. Murphy's [11] information as a jump-start, H. Hocheng et al. [7] sought to determine drilling methods that would result in zero delamination while drilling composite materials including waterjet machining. In drilling composite laminates, the uncut thickness to withstand the drilling thrust forces decreases as the drill approaches the last (exit) ply. The laminate at the bottom can be separated from the interlaminar bond around the hole edge. During this time, the loading from drilling exceeds the interlaminar bonding strength and delamination occurs, seen before in Figure 4 [11].

The main issue with waterjet machining is that damage is introduced into the working piece upon initial contact with the stream due to shock loading. Delamination can be eliminated by reducing the jet speed though, this in turn hinders the piercing capabilities. Hocheng's tests concluded that waterjet machining creates the holes fast and fine for medium to large diameter sizes in general without creating delamination. However, the initial investment is relatively high compared with traditional drilling schemes [7].

For all drilling schematics, the use of a back-up plate prevents the delamination caused by the drill exiting the piece; this is because the plate prevents the last ply from debonding as it adds an additional threshold force for delamination to begin in the first place [7].

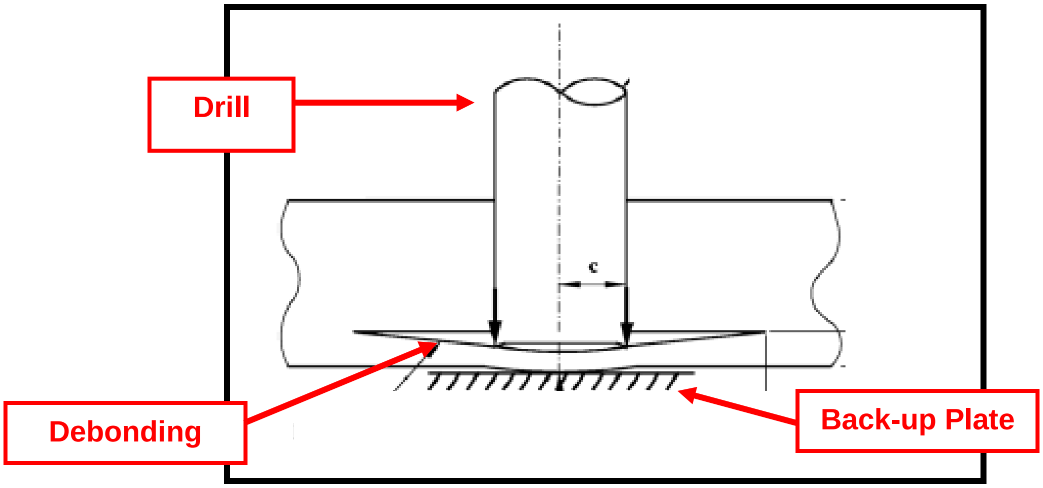

Figure 6: Circular plate model for delamination analysis, with back-up plate [7]

2.4 Thermographic Analysis of Fatigue Behaviour in Composites

L. Toubal et al. [14] completed experiments to demonstrate the relationship between the dissipation of heat and the damage of composites during fatigue testing. He completed his experiments by placing his carbon fibre epoxy composite plates in a mechanical testing device. These plates were subjected to cyclic loading and unloading while an infrared camera equipped for thermographic inspection was recording the behaviour.

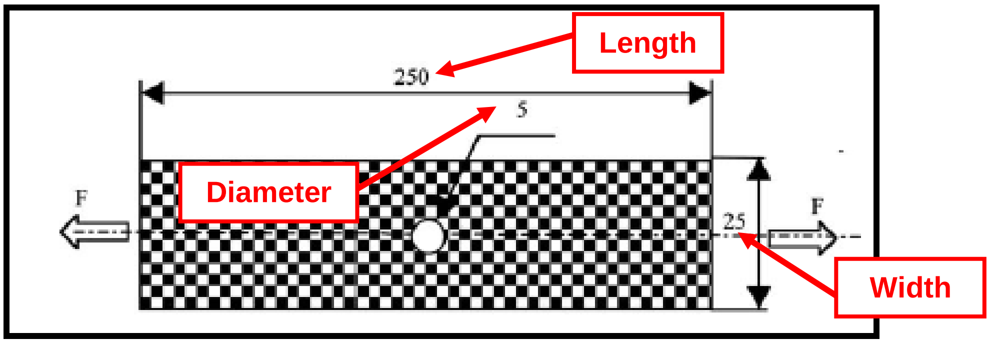

Figure 7: A schematic of the work pieces used by Toubal (units in mm) [14]

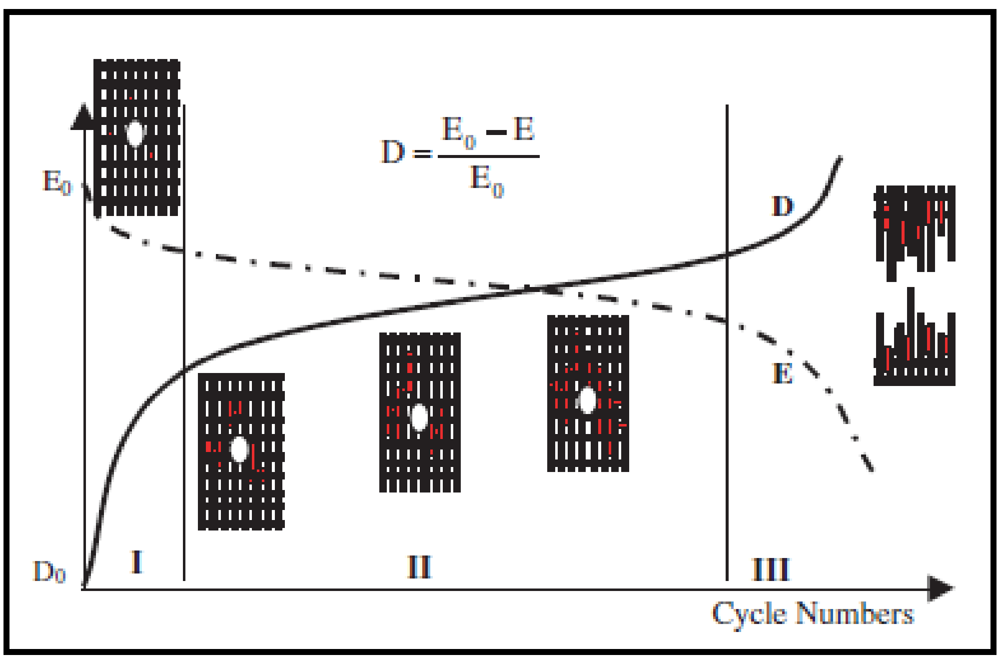

*Figure 8: Graphic displaying the evolution of cumulative damage vs. number of cycles; **'D'** represents the amount of damage damage, **'E_0'** represents the initial moduli of stiffness and **'E'** represents the residual moduli of stiffness [14]*

Based on Figure 8, one might believe lead to believe that the stiffness modulus reaches zero upon failure; this however isn't true. The moduli of stiffness prior to fracture is $\boldsymbol{E_f}$ and a new parameter ***D'*** which accounts for the total accumulated damages, incorporates it. Figure 9 below illustrates this, note that $\boldsymbol{N_f}$ is the number of cycles until failure and ***N*** is the number of cycles completed. [14]

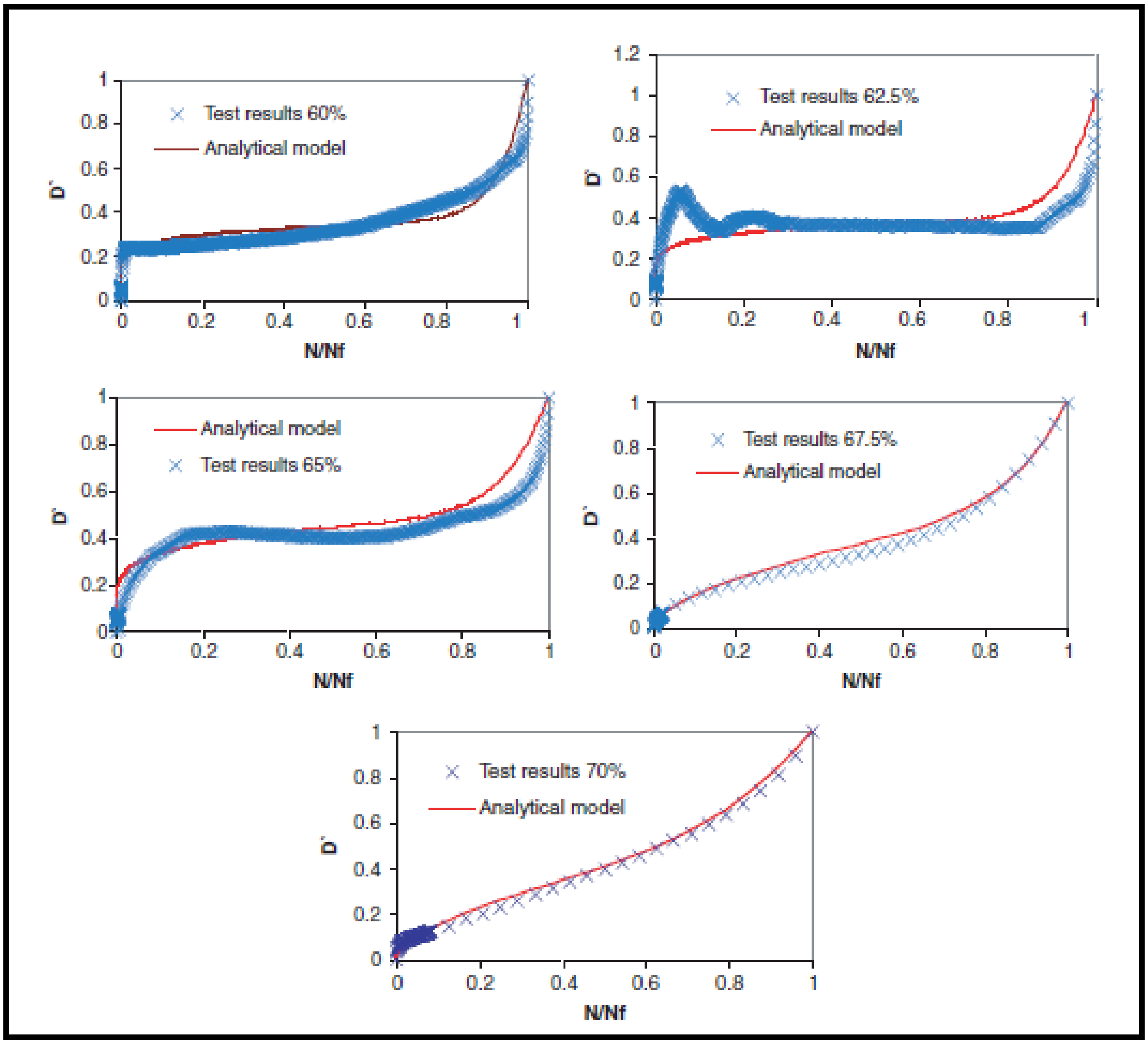

Figure 9: Toubal comprised 5 graphs that compare the evolution of damage for different load levels (as a percentage of the total strength of the material) [14]

His experimental results of the damage evolution demonstrate three different stages. The first stage, the fatigue damage grows rapidly due to the occurrence of multiple damage modes within the material. The damage increases steadily and slowly during the second stage. During the third and final stage, the damage grows rapidly due to the fracture of the fibres.

IRT can be incorporated as part of a fatigue testing procedure. As a material becomes deformed due to repeated stress loading, it releases heat as the temperature varies proportionally to the sum of the stresses [15-17]. Thermography records these changes from the infrared radiation emitted by the object [18]. During a fatigue test, the area of the specimen placed close to the gauge responsible for the loading increases in temperature as the number of cycles increases [14].

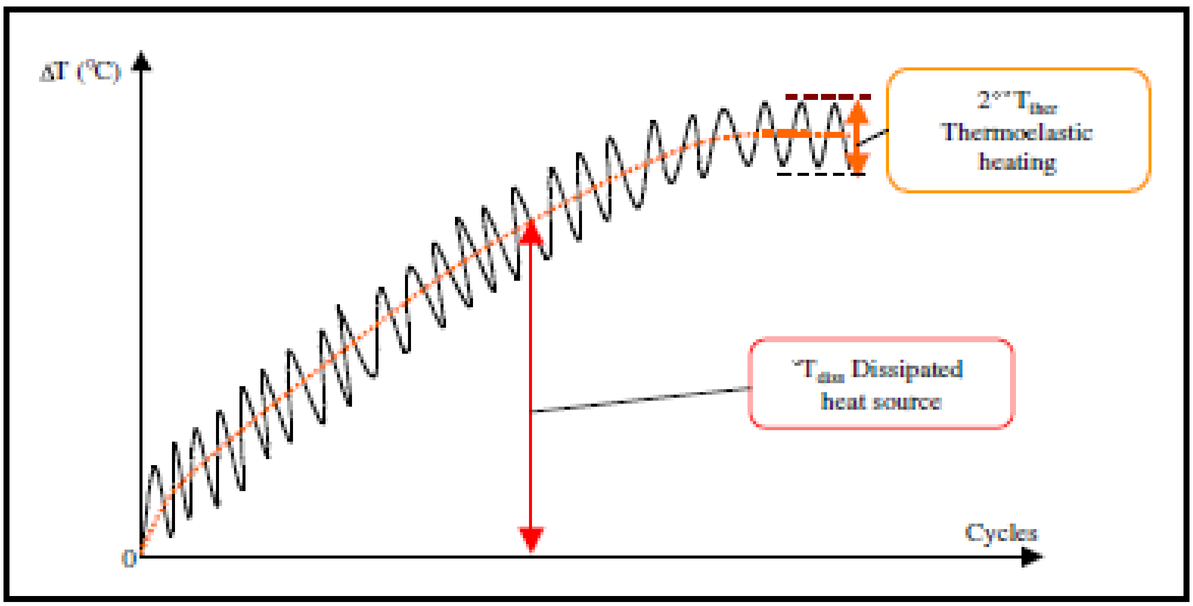

Figure 10: A schematic of the thermal evolution during a fatigue test [14]

The evolution of the temperature also appears to follow three stages [14]. In the first stage, the temperature variation is due to the frictions as the load is being applied (fibre/fibre interactions). The second stage has a temperature plateau as the damage accumulation becomes saturated. Finally, there is an abrupt increase in temperature as the workpiece becomes close to rupture.

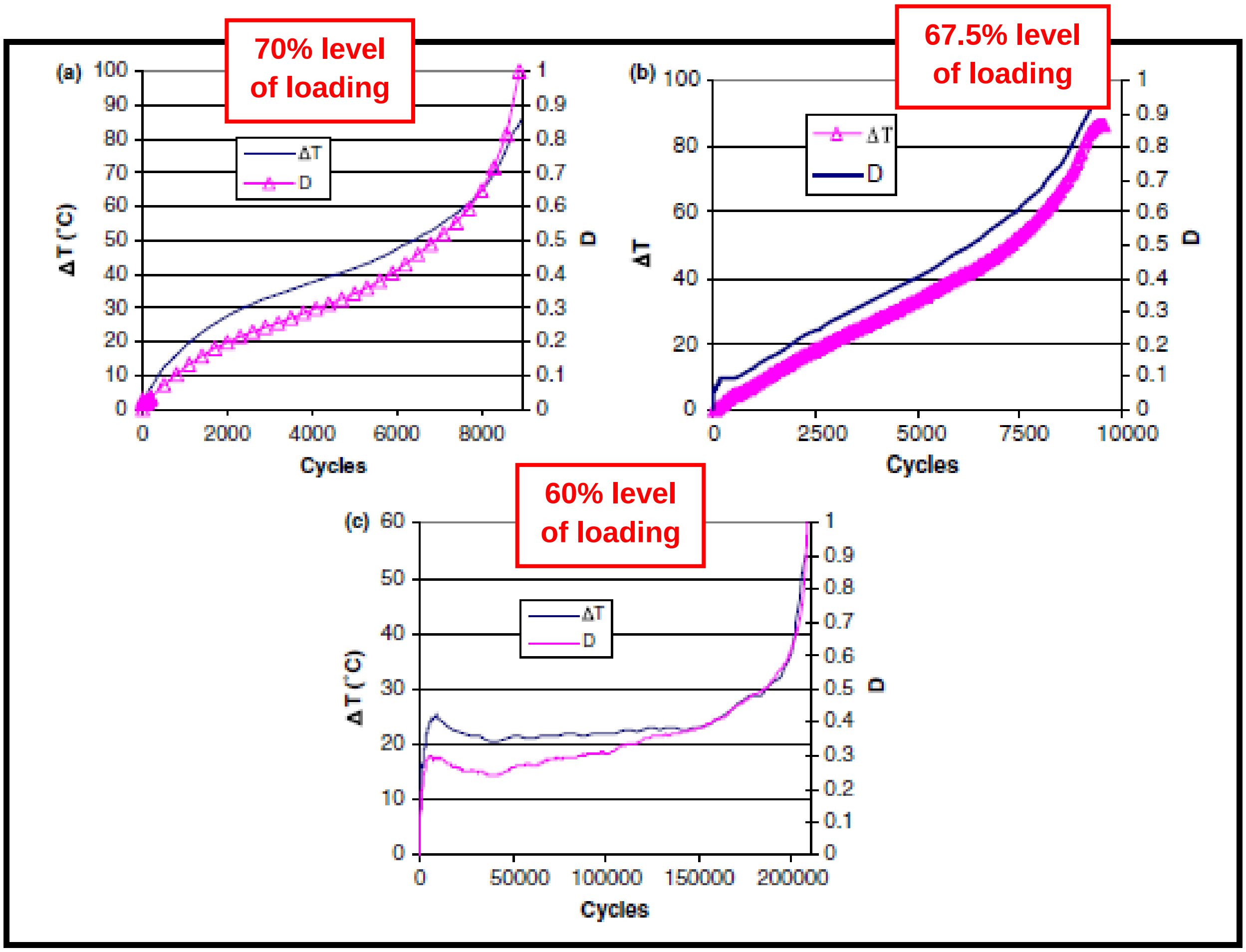

Figure 11: Comparison between the change of the temperature and the damage at different load levels (as a percentage of the total material strength), Toubal noticed that the patterns produced by both measurements were relatively similar [14]

2.5 The Effects of Ply Stack-up

Pinned joint configurations are potentially problematic to designers due to stress concentrations such that the strength of the structural member is essentially the strength of the joint. A. Aktas and H. Durikolu looked into pin loaded carbon epoxy composite laminates with different stacking sequences to analyze their maximum strength during load-bearing applications. The laminates had the following stacking sequences: [90º/45º/-45º/90º] and [90º/45º/-45º/0º], whereby the angles indicate how the fibres of each ply were aligned; both had identical properties aside from ply alignment. The results of the tests are summarized in Figure

13. Note that the ratios used as the independent variables are summarized in figure below (Figure 12). In each case, [90º/45º/-45º/0º] stacking sequence proved to have more mechanical integrity [19].

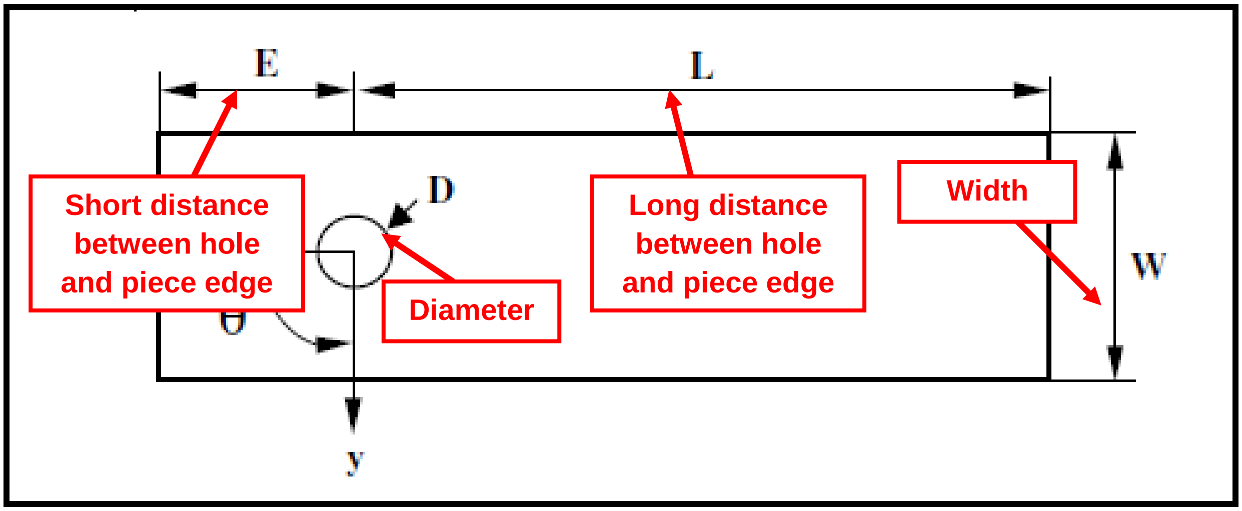

Figure 12: Schematic of the workpiece used by Aktas including defined variables [19]

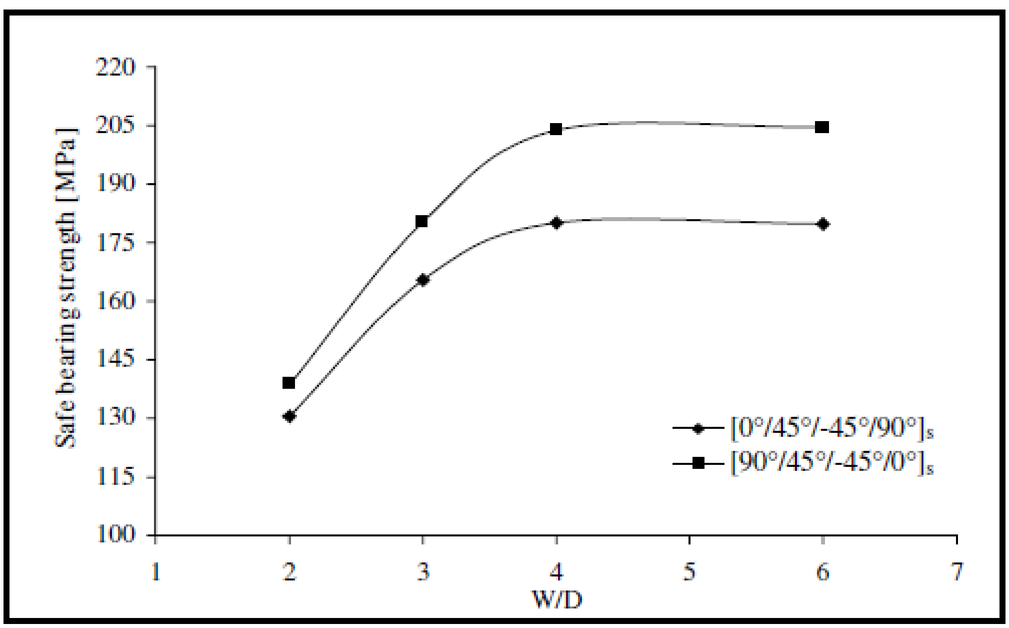

Figure 13: Graph comparing the safe net bearing strength between composites of different ply stack-up schematics [19]

Chapter 3: Materials and Procedures

This section of the report will discuss the materials and procedures used in this investigation.

3.1 Materials

Two woven 10-ply carbon-fibre epoxy plates with a stacking sequence of [+45º/-45º] have been provided by Hexcel Composites [20]. Both composite plates have the exact same dimensions, manufacturing processes, and save sized drill hole at the centre of each plate. For every plate, the length is 250 mm, the width is 25 mm, the thickness is 2.2 mm and the hole diameter is 6 mm.

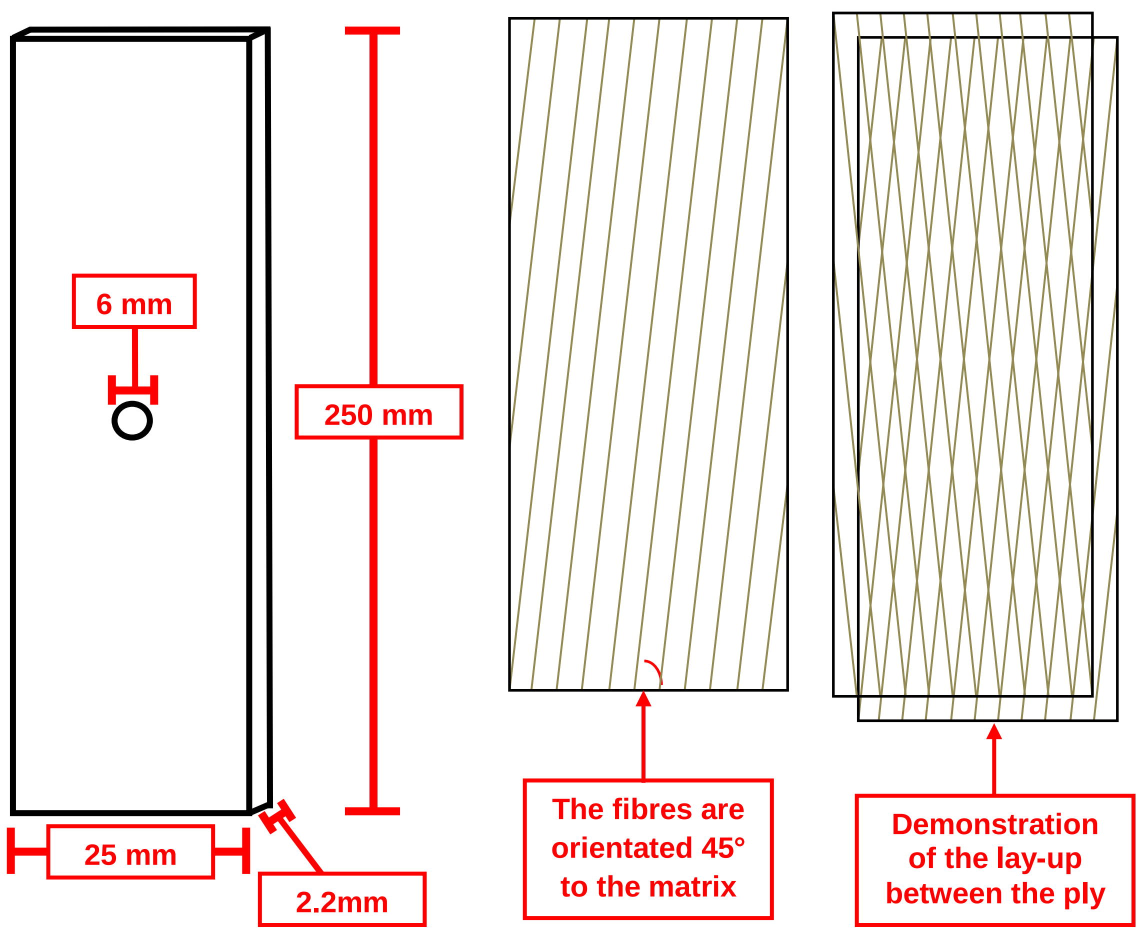

Figure 14-16: Various schematics, from left to right - dimensions of the workpieces, the fibre orientation, and the ply stack-up

The only differing factor between the plates is the hole itself: 1 plate was drilled using a tungsten carbide drill bit that had been coated with Titanium Nitride (TiN) and 1 plate was drilled using waterjet machining. The plate that had been machined use traditional drilling are referenced as Hexply T2H 268 150 EH25 NS 35% (noted as T2H-EH25) with a 59% fibre content and 0.25 mm thick ply. The plate that had been machined using waterjet drilling is referenced as Hexply T700GC 268 M21 34% (noted T700-M21) with a 58% fibre content and a 0.26 mm ply [20].

3.2 Strain Gauge Procedure

Prior to placing the gauges on the plates, both plates were scrubbed with 400-grit silicon carbide paper to remove any surface particles (such as dust, sand, or dirty), doing so ensures that the gauges are placed flat against the surface. M-Prep conditioner was applied to the plate surface to remove any residues and the conditioner was scrubbed off with cotton swaps. Four gauges were applied to the centre of each plate, approximately 10 mm from each side of the hole with M-Bond 200 Catalyst and allowed to dry for 30 seconds. The gauges were sealed to the plate by placing cellophane tape to the outside of each gauge. Colour-coded lead wires were used in this experiment (red, black and white), the black and white wires were exposed with pliers and soldered together. The four gauges were connected to each of the channels of a DSub-15-pin Connectors. The DSub-15-pin connectors were placed in the CRONOS-PL2 which was connected to a laptop that had been installed with FAMOS V5.0 to control the amount of strain induced; the plates were subjected to dynamic tensile loads of 2000 N and 2500 N.

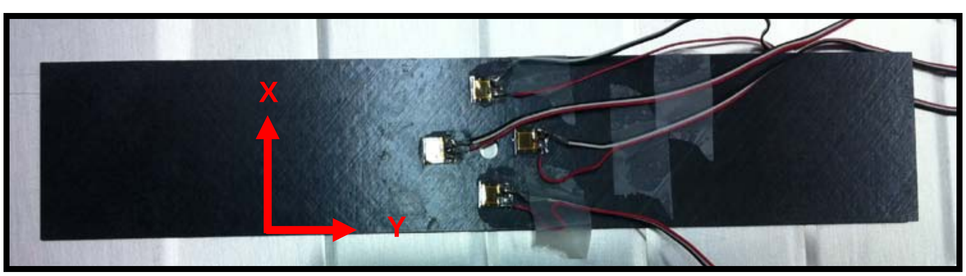

Figure 17: Gauge and wiring positioning on plate prior to testing

3.3 Infrared Thermography Analysis Procedure

The plates were scrubbed with 400-grit silicon carbide paper to remove surface residues such as dirt and dust particles. An extensometer was fixed on the gauge-length section of the plate to record the value of the stress and store them directly into the acquisition system for further analysis. Each plate was locked into the Instron 8874 mechanical tester with its back side facing the camera. The thermal camera and its respective tripod were placed approximately 1 m away. The upper jaw of the Instron 8874 mechanical tester supplied the load, and cyclic loads of 2000 N and 2500 N at a frequency of 5 Hz and for 10,000 cycles.

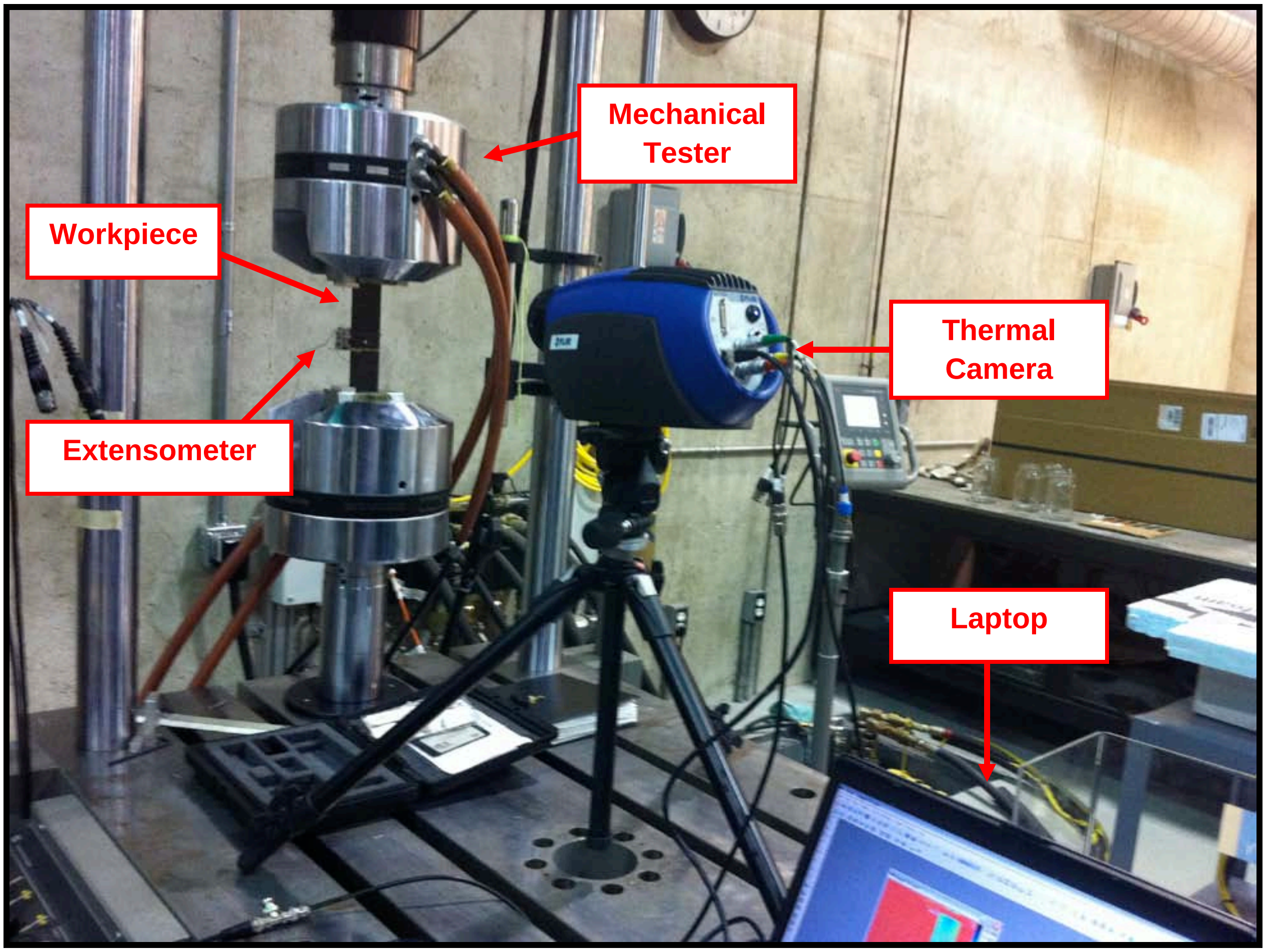

Figure 18: Labeled thermography experimentation set-up

3.4 Tensile Testing Procedure

The tension tests were done by collaborators of the Bougherara group at the University of Québec at Trois Riviérés. The team used these plates and tested them until fracture to develop stress-strain curves. The purpose of these tests was to gain basic mechanical properties of the materials and determine the fracture direction.

Chapter 4: Results Analysis

This section of the report will provide key quantitative results obtained through the various tests done to these plates.

4.1 Strain Gauge Results

The plates that had been drilled with the coated drill bit and through waterjet underwent strain gauge testing. Figure 19 illustrates the results, which were tabulated by averaging the two readings received on the X-direction gauges (see Figure 17). At a higher load level, the waterjet drilled plate accumulated less stress. At a lower load level, the bit drilled plate accumulated less stress. Y-direction gauges were not analyzed as thermography analysis did not take that direction into consideration.

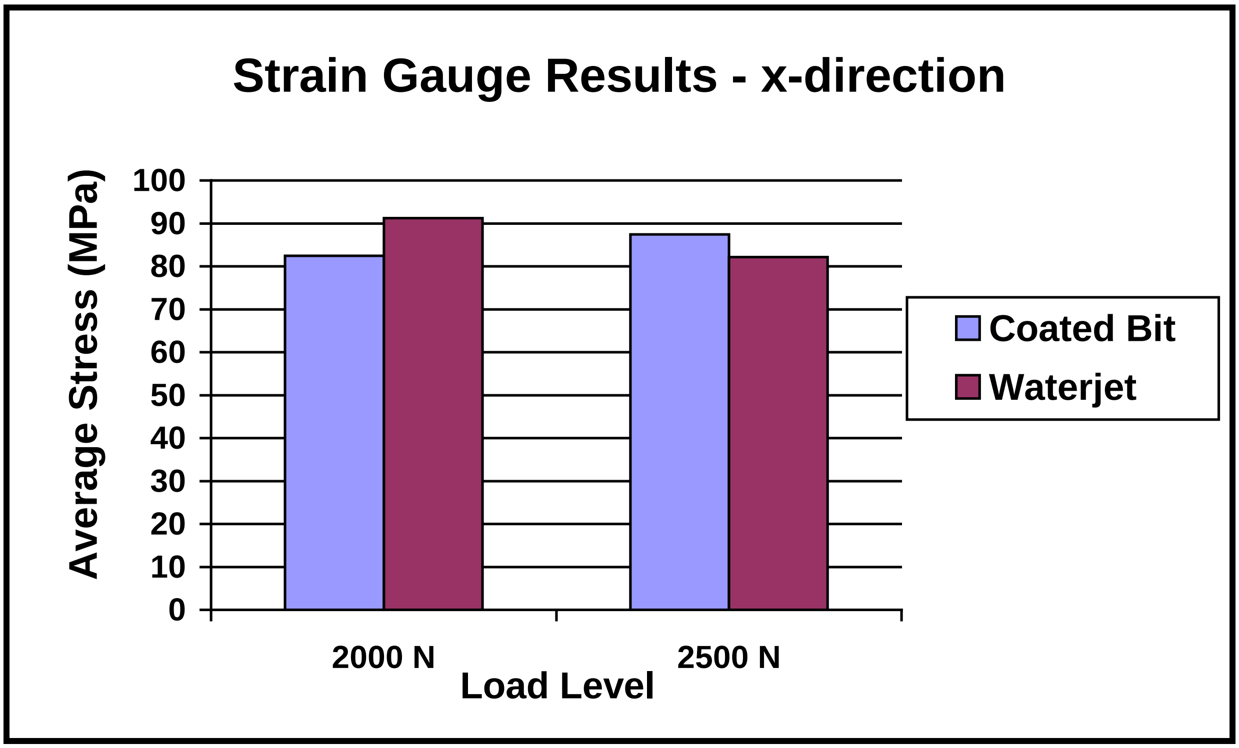

Figure 19: Chart comparing the stress obtained by carbon epoxy plates during strain gauge testing - coated drill bit machined and waterjet machined

4.2 Infrared Thermography Results

The plates were analyzed through infrared thermography while undergoing cyclic loading at loads of 2000 N and 2500 N for a total of 10,000 cycles. Altair Software was used to analyze the images captured by the thermal camera; the technique can be seen in Figures 22 and 23. Altair allowed observation of the variation in both peak stress levels and temperature difference across the area of the plate with the machined hole. Below is a chart comparing the peak stress levels recorded for the two plates; the results obtained are very similar to that obtained by strain gauge testing. There appears to be no significant pattern in stress accumulation comparing the two plates.

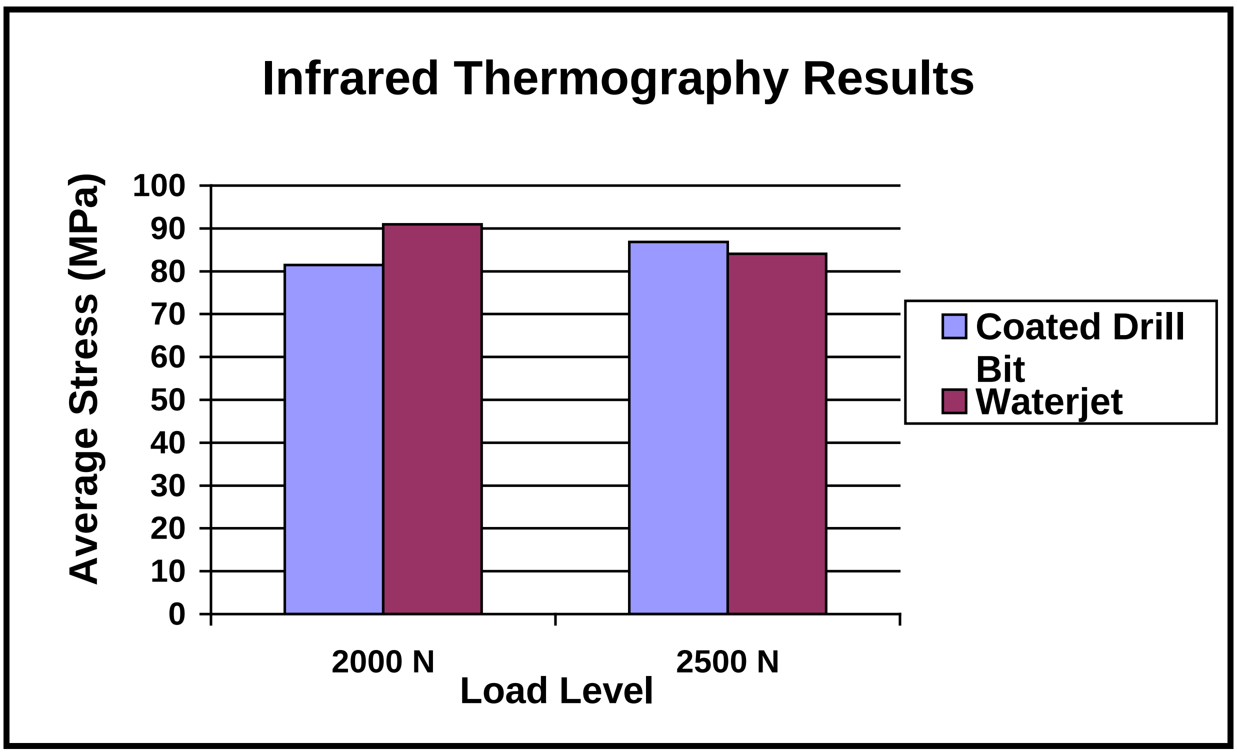

Figure 20: A chart comparing the maximum stress level achieved by the plates (closest to the hole) when loaded at 2,000 N and 2,500 N for 10,000 cycles

When comparing the temperature variation across the machined plates, the highest temperature change was noted in the areas closest to the hole. Though, the temperature variation peak was similar in both peaks, as seen in Figure 21 below.

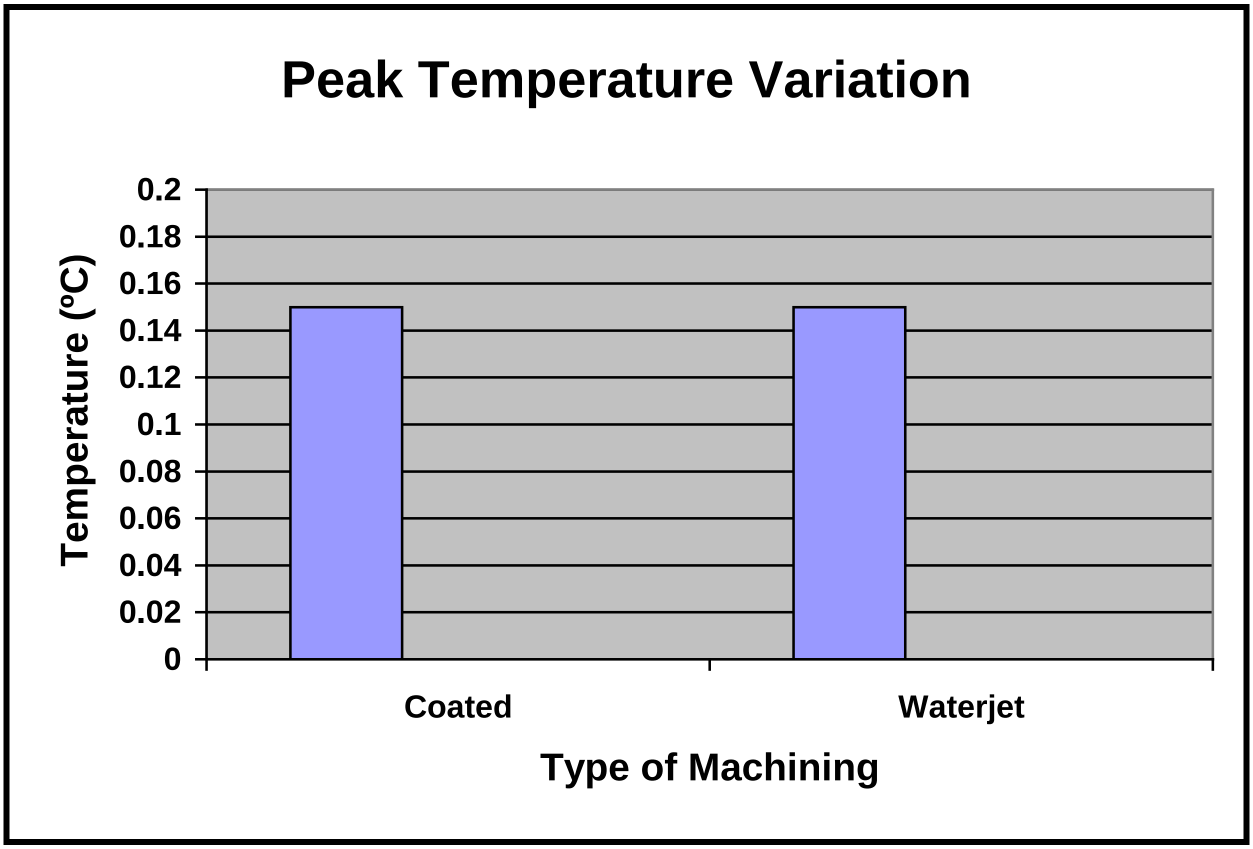

Figure 21: A chart comparing the maximum temperature increase achieved by the plates (closest to the hole) when loaded at 2000 N and 2500 N for 10,000 cycles (the values were identical for both load levels)

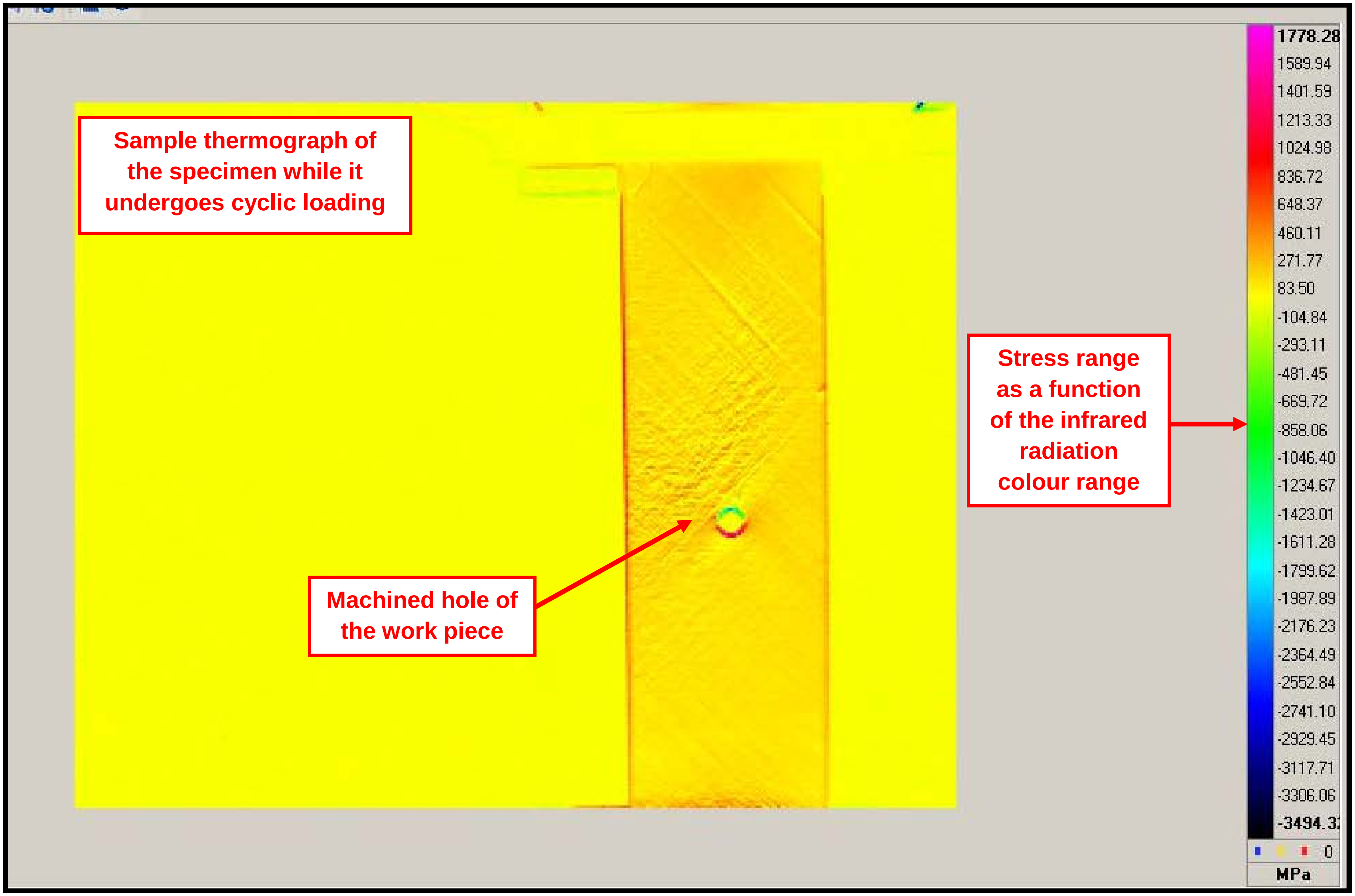

Figure 22: Sample thermograph obtained by Altair

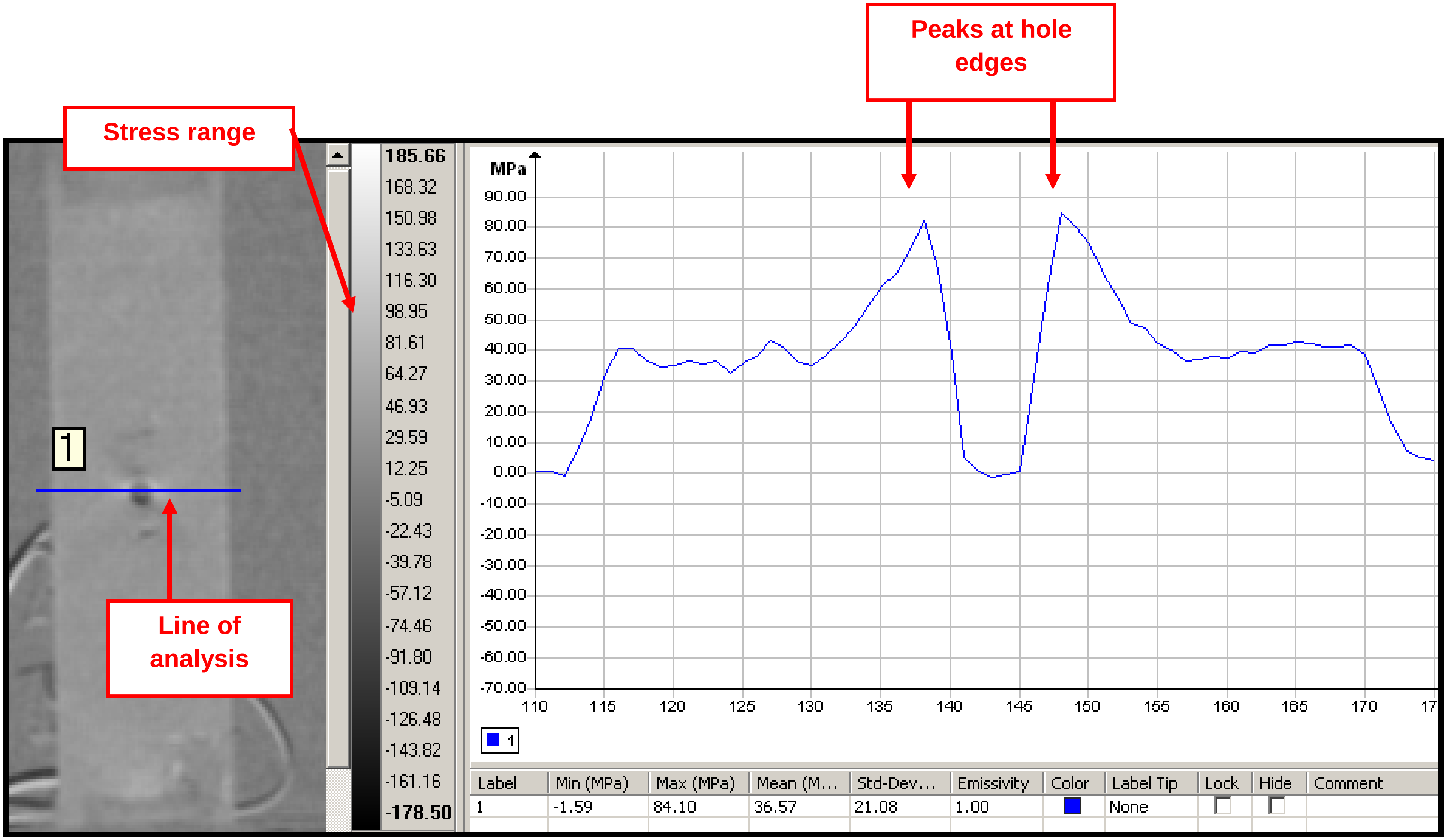

Figure 23: Sample analysis technique used to compare the stress and temperature variation across the width of the plates containing a machined hole

4.3 Tension Tests Results

Below is the stress-strain curves produced by both plates undergoing tensile-testing until fracture. The tension tests results do not demonstrate a significant difference that may suggest that one machining method results in a more structurally resilient component. The workpiece machined with the coated bit did withstand a higher force and strain prior to fracture than the workpiece machined through waterjet. Images were captured during the process; interestingly, the images demonstrate that the fracture process did not occur adjacent to the holes in either workpiece, but rather with the ply orientation, seen in Figure 25. Prior to the fracture, both plates demonstrate fibre breakage near the hole, seen in Figure 26.

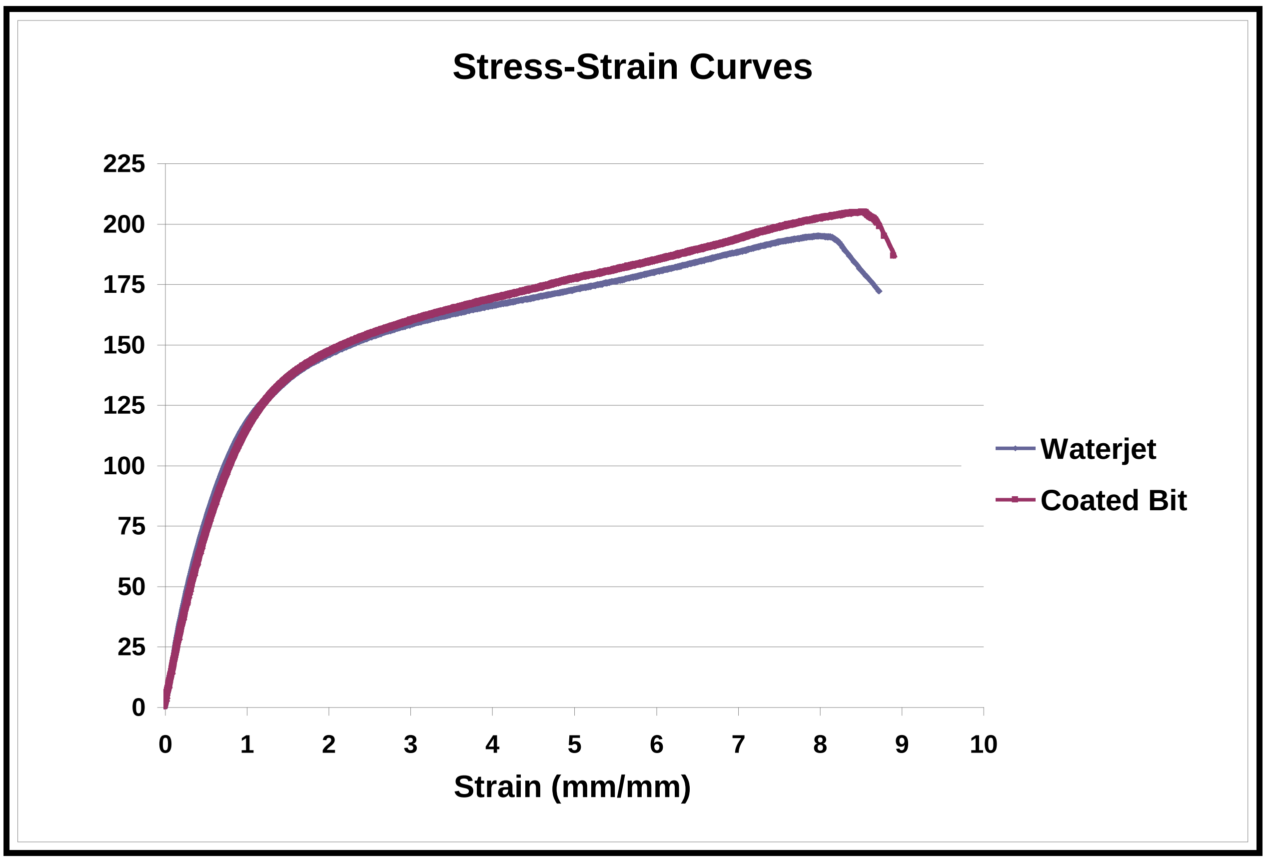

Figure 24: Results obtained from tensile-testing both workpieces until fracture

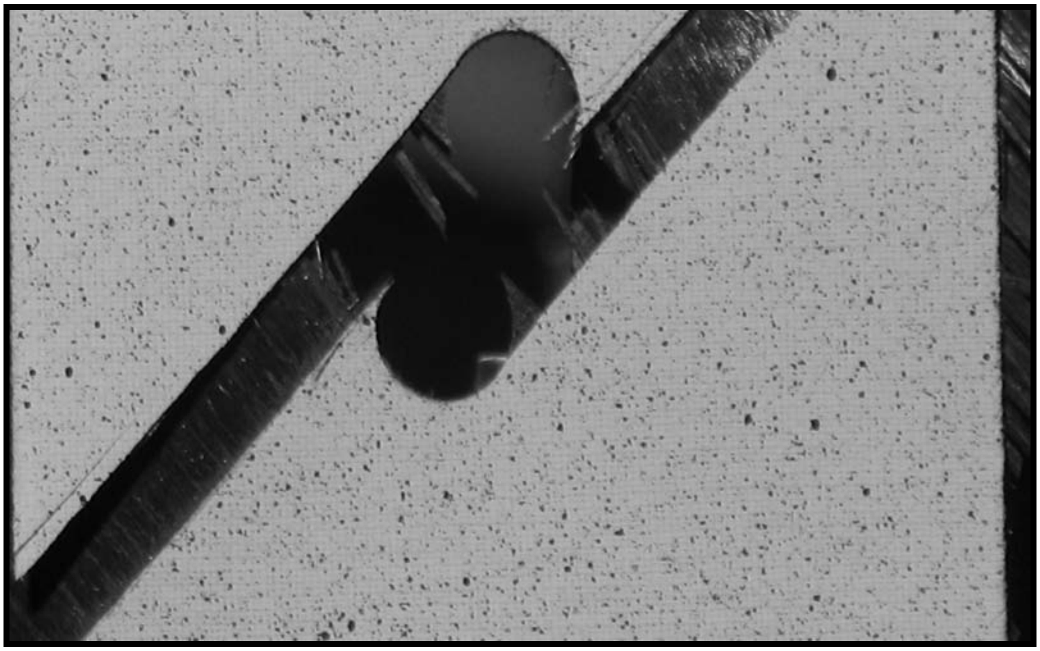

Figure 25: Final fracture of the waterjet machined plate demonstrating that the fracture pattern follows the ply alignment

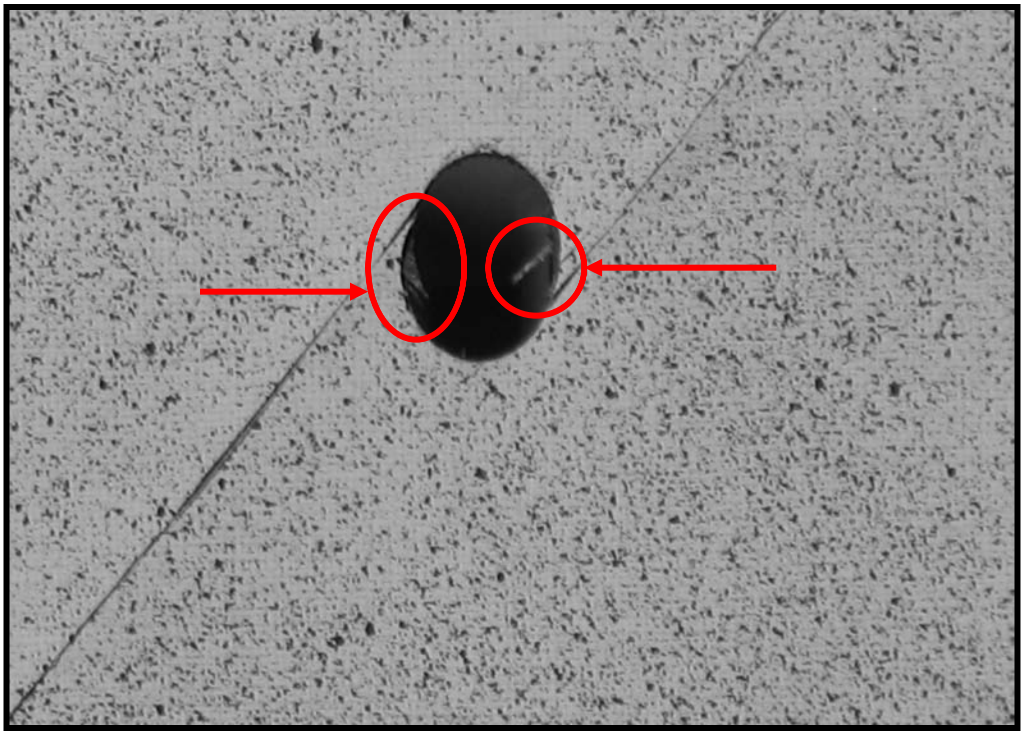

Figure 26: Fibre breakage prior to fracture

Chapter 5: Conclusion and Future Work

The purpose of this lab report was to compare the effects of machining methods on composite plates in terms of their behaviours in load-bearing conditions. The three testing methods utilized in this investigation do not demonstrate enough evidence suggesting one machining method is beneficial over the other thus far. The strain gauge testing and infrared thermography analysis during cyclic loading provided similar figures and minor differences between the workpieces. This validates the infrared thermography testing as a form of non-destructive testing. Tension tests do not provide a significant basis of comparison between the two drilling mechanisms.

Aerospace applications rely on longevity of their components, as such, future work may want to analyze these materials through fatigue testing. Rather than investigating the stress concentrations at specific load levels, the plates should be tested at continuously increasing load levels at a specific number of cycles until fracture. Doing so would allow comparison of damage evolution and how the stiffness of the plates deteriorates with increasing load levels. The practice of IRT for these investigations should continue as it has the potential to supply information for the evaluation of the extension of the impact damage and detailed imaging that could lead into a better understanding of metal and fibre layers in material hybrids.

As of now, the only beneficial factor regarding waterjet machining is the speed and ease of automation and use. Future investigation may want to focus on the level of delamination and the economic feasibility of implementing non-traditional cutting techniques to create holes for bolted joint connections. Future work should continue to make use of infrared thermographic analysis as it provides colourful images of the stress accumulation and can provide vital hints towards where the fracture will occur and also make known of where fibre-breakage persists.

References

[1] Michael F. Ashby, *Materials Selection in Mechanical Design,* 3rd Edition. Burlington, Massachusetts: Butterworth Heinemann Inc., 2005.

[2] *Basic Properties of Reference Crossply Carbon-Fiber Composite*. Prepared by the Oak Ridge National Laboratory in February 2000 for the U.S. Department of Energy.

[3] William D. Callister, *Fundamentals of Materials Science and Engineering,* 2nd Edition. The University of Utah: John Wiley & Sons, Inc., 2005.

[4] H. Mao, S. Mahadevan, "Fatigue damage modeling of composite materials," *Composite Structures*, vol. 58, 2002, pp. 405-410. [Online]. Available: http://www.elsevier.com

[5] Bob Matthews, *Applied Stress Analysis XI - Composite Materials (Analysis),* presented in August 1971 for General Dynamics - Convair Division. [Online]. Available: http://www.jstor.org/stable/2417657.

[6] L. Toubal, M. Karama, and B. Lorrain, "Stress concentration in a circular hole in composite plate", *Composite Structures*, vol. 68, 2005, pp. 31-36. [Online]. Available: http://www.sciencedirect.com.

[7] H. Hocheng, C.C. Taso, "the path towards delamination-free drilling of composite materials," *Journal of Materials Processing Technology*, vol. 167, 2005, pp. 251-264. [Online]. Available: http://www.elsevier.com/locate/jmatprotec.

[8] “Overview of Waterjets”, Waterjets.org. 2011. [Online]. Available: http://www.webcitation.org.

[9] “Waterjet Cutting”, John W. Sutherland’s Research Page. 2011. [Online]. Available: http://www.mfg.mtu.edu/

[10] S. D. Pandita, K. Nishiyabu, and I. Verpoest, "Strain concentrations in woven fabric composites with holes," *Composite Structures*, vol. 59, 2003, pp. 361-368. [Online]. Available: http://www.elsevier.com.

[11] C. Murphy, G. Byre, and M.D. Gilchrist, “The performance of coated tungsten carbide drills when machining carbon fibre-reinforced epoxy composite materials,” Journal of Engineering Manufacture, vol. 216, no. 2, pp. 143-152. 2002. [Online]. Available: http://www.pib.sagepub.com.

[12] “High-performance Carbide Drill Bits,” Cutting Tool Central by American Machinist. 2011. [Online]. Available: http://www.cutting-tool.americanmachinist.com.

[13] “Super Primalloy Drill Bits”, Kimball Midwest Product Information Sheet. July 1996. [Online]. Available: http://www.kimballmidwest.com.

[14] L. Toubal, M. Karama, and B. Lorrain, "Damage evolution and infrared thermography in woven composite laminates under fatigue loading," *International Journal of Fatigue*, vol. 28, January 2006, pp. 1867-1862. [Online]. Available: http://www.sciencedirect.com.

[15] C. Meola, G. M. Carlomagno, A Squillace, A. Vitiello, “Non-destructive evaluation of aerospace materials with lock-in thermography”, *Engineering Failure Analysis*, vol. 13, 2006, pp. 380-388. [Online]. Available: http://www.sciencedirect.com

[16] D. Bates, G. Smith, D. Lu, and J. Hewitt, "Rapid thermal non-destructive testing of aircraft components", *Composites: Part B*, vol. 31, 2000, pp. 175-185. [Online]. Available: http://www.elsevier.com.

[17] J.A. Charles, F. J. Appl, and J.E. Francis, "Using the Scanning Infrared Camera in Experimental Fatigue Studies," *Experimental Mechanics*, vol. 15, no. 4, 1975, pp. 133-138. [Online]. Available: http://www.springerlink.com.

[18] Maldague X. P. V., Jones T. S., Kaplan H., Marinetti S. and Prystay M. "Chapter 2: Fundamentals of Infrared and Thermal Testing: Part 1. Principles of Infrared and Thermal Testing", in *Nondestructive Handbook, Infrared and Thermal Testing*, Volume 3, 3rd edition, Columbus, Ohio, ASNT Press, 2001.

[19] A. Aktas, M. H. Dirikolu, “The effect of stacking sequence of carbon epoxy composite laminates on pinned-joint strength,” Composite Structures, vol. 62, 2003, pp. 107-111. [Online]. Available: http://www.elsevier.coim/locate/compstruct.

[20] “The World of Composite Technologies”, Hexcel. 2011. [Online]. Available: http://www.hexcel.com.